

Checking the reliability of equivalent width R_{23} for estimating the metallicities of galaxies

Y. C. Liang^{1,2}, F. Hammer², and S. Y. Yin^{1,3,4}

¹National Astronomical Observatories, Chinese Academy of Sciences, 20A Datun Road, Chaoyang District, Beijing 100012, China

²GEPI, Observatoire de Paris-Meudon, 92195 Meudon, France

³Department of Physics, Hebei Normal University, Shijiazhuang 050016, China

⁴Department of Physics, Harbin University, Haerbin 150086, China

Received; accepted 8 August 2007

ABSTRACT

Aims. We verify whether the O/H abundances of galaxies can be derived from the equivalent width (EW) R_{23} instead of the extinction-corrected flux R_{23} , and eventually propose a method of improving the reliability of this empirical method, which is often used for the non-flux calibrated spectra of galaxies.

Methods. We select 37,173 star-forming galaxies from the Second Data Release of the Sloan Digital Sky Survey (SDSS-DR2), which offers a wide range of properties to test the EW method.

Results. The EW- R_{23} method brings with it a significant bias: for the bulk of SDSS galaxies, it may affect the determination of $\log(\text{O}/\text{H})$ by factors ranging from -0.2 to 0.1 dex and for some galaxies by factors ranging from -0.5 to 0.2 dex. We characterize this discrepancy (or bias) by $\alpha = (I_{[\text{OII}]} / I_{\text{H}\beta}) / (\text{EW}_{[\text{OII}]} / \text{EW}_{\text{H}\beta})$, which is virtually independent of dust extinction, while tightly correlating with $D_n(4000)$, although at a lower significance, with $(g - r)$ colors.

Conclusions. The EW- R_{23} method cannot be used as a proxy for the extinction-corrected flux R_{23} method. From analytical third-order polynomial fits of α versus $(g - r)$ colors, we have been able to correct the EW- R_{23} method. With this additional and easy correction, the EW- R_{23} method provides O/H abundance values similar to those derived from the extinction-corrected flux R_{23} method with an accuracy of ± 0.1 dex for $>92\%$ of the SDSS galaxies.

Key words. Galaxy: abundances - Galaxies: evolution - Galaxies: ISM - Galaxies: photometry - Galaxies: spiral - Galaxies: starburst

1. Introduction

Chemical abundance is a fundamental parameter for tracing the history of star formation and evolution of galaxies. Oxygen is the most commonly used metallicity indicator in the interstellar medium (ISM) by virtue of its high relative abundance and strong emission lines in the optical part of the spectrum (e.g., $[\text{O II}]\lambda 3727$ and $[\text{O III}]\lambda\lambda 4959, 5007$). However, the “direct” method of estimating oxygen abundances from electron temperature (T_e) is generally only available for metal-poor galaxies ($12 + \log(\text{O}/\text{H}) < 8.5$), where the $[\text{O III}]\lambda 4363$ emission line can possibly be detected, which is needed for measuring T_e by its ratio to $[\text{O III}]\lambda\lambda 4959, 5007$ (Pagel et al. 1992; Skillman & Kennicutt 1993). For metal-rich galaxies, the most commonly used are empirical strong-line methods, such as R_{23} :

$$R_{23} = \frac{I([\text{OII}]\lambda 3727) + I([\text{OIII}]\lambda\lambda 4959, 5007)}{I(\text{H}\beta)}, \quad (1)$$

i.e. the flux ratios of $[\text{O II}]$ and $[\text{O III}]$ to $\text{H}\beta$ (Pagel et al. 1979; McGaugh 1991; Zaritsky et al. 1994; Kobulnicky et al. 1999; Tremonti et al. 2004 and the references therein).

However, flux calibrations are frequently problematic in the current generation of wide-field galaxy surveys of multiobject spectrography, because of unfavorable observing conditions or instrumental effects such as a variation in system response over the field of view, nevertheless, one still expects to derive metallicity properties of the star-forming galaxies detected in the large

data sets from surveys. Then, *equivalent widths* (EWs) are being used to replace the fluxes of their R_{23} values for estimating metallicities of the galaxies, i.e., from the EW R_{23} :

$$\text{EW } R_{23} = \frac{\text{EW}([\text{OII}]\lambda 3727) + \text{EW}([\text{OIII}]\lambda\lambda 4959, 5007)}{\text{EW}(\text{H}\beta)}. \quad (2)$$

This replacement was first checked by Kobulnicky & Phillips (2003; KP03 hereafter) on the basis of a sample of 243 nearby galaxies. Consequently, this method has been used by some researchers to estimate metallicities of nearby and even intermediate- z galaxies (e.g. Kobulnicky et al. 2003; Kobulnicky & Kewley 2004; Lamareille et al. 2005a,b; Mouhcine et al. 2006a,b etc.).

However, it is known that there is a continuum ($F_{C\lambda}$) scale factor between the flux (F_λ) and EW (W_λ) values of the emission line:

$$W_\lambda = \frac{F_\lambda}{F_{C\lambda}}. \quad (3)$$

This will naturally make us ask whether the continua underlying $[\text{O II}]$ and $\text{H}\beta$ (and $[\text{O III}]$) are very similar or not. If not, $F_{C\lambda}$ could be far from a unique constant, and then the metallicities derived from EW R_{23} could have large discrepancies from those derived from flux R_{23} .

The SDSS provides a complete dataset and measurements up to several ten-thousand galaxies, making it a very good database for studying this question. In this paper, we selected 37,173 star-forming galaxies from the SDSS-DR2 to further check the reliability of using EW R_{23} replacing the extinction-corrected flux

R_{23} to estimate the metallicities of galaxies. Moreover, this is a large homogeneous database observed by one single highly efficient facility, which will minimize the effect of using various instruments. Some other characteristic parameters provided by the SDSS can also help for understanding the question further, e.g., $D_n(4000)$, g and r photometric magnitudes, etc.

This paper is organized as follows. The sample selection criteria are described in Sect.2. In Sect.3, we check how big the difference is between the underlying continua of [O II] and $H\beta$, which is quantified as a parameter α (by $1/\alpha$). The emission-line quantities of the sample galaxies are analyzed in Sect.4, as well as the discrepancies between their EW R_{23} and flux R_{23} , and the discrepancies between the derived $\log(O/H)$ abundances from them. In Sect.5, we try to find the factors that mostly affected the α parameter, then to find the relations between them and α , hence to modify the EW R_{23} method, which includes the stellar population indicators $D_n(4000)$ and colors. In Sect.6, we discuss the boundary of the upper branch of $12+\log(O/H)$ abundances from the $\log R_{23}$ calibration, then summarize and conclude this paper in Sect.7.

2. Sample selection

The data analyzed in this study were drawn from the SDSS-DR2 (Abazajian et al. 2004). These galaxies are part of the SDSS ‘‘main’’ galaxy sample used for large-scale structure studies (Strauss et al. 2002). We selected a sample of star-forming galaxies with metallicity estimates from the SDSS-DR2 database. The selection criteria are similar to those of Tremonti et al. (2004) and Liang et al. (2006). We summarize the criteria for selection as follows, and mark the selected number of the sample galaxies in parenthesis at the end of each step:

- (i) SDSS-DR2 (261,054), $14.5 < r < 17.77$ mag (Petrosian magnitude, 193,890 left);
- (ii) $12+\log(O/H)_{SDSS} > 0$ (50,385 left) (SDSS refers to the metallicity values provided by the MPA/JHU group, which were obtained on the basis of the 2001 Charlot & Longhetti model and Bayesian technique, see Tremonti et al. 2004);
- (iii) $0.04 < z < 0.25$ (40,693 left) (this allows the spectral coverage from [O II] $\lambda 3727$ to [S II] $\lambda 6731$ for the sample galaxies);
- (iv) the emission lines [O II], $H\beta$, [O III], $H\alpha$, and [N II] are detected and their fluxes and EWs are reasonable; fluxes of emission lines $H\beta$, $H\alpha$, and [N II] $\lambda 6584$ are detected at levels higher than 5σ (39,029 left);
- (v) $8.5 < 12+\log(O/H)_{R_{23}} < 9.3$ (38,932 left) (we adopt the formula of Tremonti et al. 2004 to convert R_{23} to the oxygen abundance $12+\log(O/H)_{R_{23}}$, which is only suitable for metal-rich galaxies; therefore, we only select the galaxies with $12+\log(O/H) > 8.5$ here; 9.3 is almost the upper limit of the abundances in the samples);
- (vi) the discrepancy between $\log(O/H)_{R_{23}}$ and $\log(O/H)_{SDSS}$ is less than 0.1 dex (37,173 left finally), which removes some scattered data points from the R_{23} calibration, as shown by Fig. 1.

Finally, we obtained a sample of 37,173 star-forming galaxies from the SDSS-DR2 as our sample in this study.

The criteria (i)-(iv) are almost the same as what was adopted in Tremonti et al. (2004), except the lower limit for redshift z was increased from 0.005 to 0.04 by following Kewley et al. (2005) to minimize the aperture effects of the SDSS. In Sect. 6, we discuss criterion (v) in particular, i.e. $12+\log(O/H) \sim 8.5$ as the lower boundary of the upper branch of oxygen abundances from $\log R_{23}$ calibration.

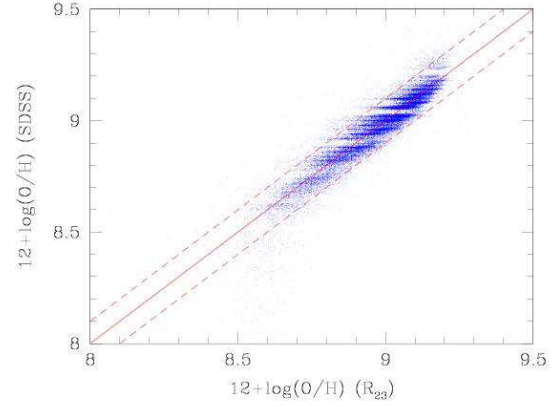


Fig. 1. Comparison between the oxygen abundances obtained by the MPA/JHU group (marked as ‘SDSS’) and those derived from R_{23} calibration of Tremonti et al. (2004) (marked as ‘ R_{23} ’). The dashed lines mark the 0.1 dex discrepancies from the equal values (solid line).

3. Quantifying the difference between EW R_{23} and flux R_{23} : determining the α parameter

The MPA/JHU collaboration has put the measurements of emission-lines and some physical parameters for a large sample of SDSS galaxies on the MPA SDSS website¹ (Kauffmann et al. 2003; Brinchmann et al. 2004; Tremonti et al. 2004 etc.). These measurement values were obtained from the stellar-feature subtracted spectra with the spectral population synthesis code of Bruzual & Charlot (2003).

Fluxes of the emission lines should be corrected for dust extinction, so we estimate the attenuation of the sample galaxies using the Balmer line ratio $H\alpha/H\beta$ and assuming case B recombination, with a density of 100 cm^{-3} , a temperature of 10^4 K , and the intrinsic $H\alpha/H\beta$ ratio of 2.86 (Osterbrock 1989), following the relation of

$$\left(\frac{I_{H\alpha}}{I_{H\beta}}\right)_{obs} = \left(\frac{I_{H\alpha 0}}{I_{H\beta 0}}\right)_{intr} 10^{-c(f(H\alpha)-f(H\beta))}. \quad (4)$$

Using the average interstellar extinction law given by Osterbrock(1989), we obtain $f(H\alpha) - f(H\beta) = -0.37$. For the data points with $c < 0$, $c = 0$ is assumed since their intrinsic $H\alpha/H\beta$ may be lower than 2.86 if their electron temperature is high (Osterbrock 1989).

Then, the extinction-corrected R_{23} parameter and its relation with the EW R_{23} are:

$$\begin{aligned} R_{23} &= \frac{I_{[OII]} + I_{[OIII]}}{I_{H\beta}} \\ &= \frac{F_{[OII]}}{F_{H\beta}} 10^{c(f([OII])-f(H\beta))} + \frac{F_{[OIII]}}{F_{H\beta}} 10^{c(f([OIII])-f(H\beta))} \\ &= \frac{W_{[OII]} F_{C,[OII]}}{W_{H\beta} F_{C,H\beta}} 10^{c(f([OII])-f(H\beta))} \\ &\quad + \frac{W_{[OIII]} F_{C,[OIII]}}{W_{H\beta} F_{C,H\beta}} 10^{c(f([OIII])-f(H\beta))} \\ &= \frac{\alpha W_{[OII]} + W_{[OIII]}}{W_{H\beta}}, \end{aligned} \quad (5)$$

where $\alpha = \frac{(F_{C,[OII]}/F_{C,H\beta}) 10^{c(f([OII])-f(H\beta))}}{(F_{C,[OIII]}/F_{C,H\beta}) 10^{c(f([OIII])-f(H\beta))}}$, and $(F_{C,[OIII]}/F_{C,H\beta}) 10^{c(f([OIII])-f(H\beta))}$ is about equal to 1 since

¹ <http://www.mpa-garching.mpg.de/SDSS/>

[O III] $\lambda\lambda 4959, 5007$ and $H\beta$ are very close in wavelength. The expression $I_{[\text{O III}], [\text{O III}], H\beta}$ refers to the dereddened, calibrated flux values of the corresponding lines; $F_{[\text{O III}], [\text{O III}], H\beta}$ refers to the observed flux values; and $W_{[\text{O III}], [\text{O III}], H\beta}$ represents the EW values of the related emission lines. The parameter c is the extinction coefficient. (Also see KP03)

The α values of these SDSS galaxies can be calculated directly from $\alpha = (F_{C, [\text{O III}]} / F_{C, H\beta}) 10^{c(f([\text{O III}]) - f(H\beta))}$, where $F_{C, [\text{O III}]}$ and $F_{C, H\beta}$ can be estimated from their ratios of fluxes to EW values, and c is the extinction coefficient. The derived α parameters of these sample galaxies show a median value of 0.85 and an average value of 0.86 in a range from 0.1 to 2.6. KP03 estimate the typical value of the α parameters of their 243 sample galaxies to be $\alpha = 0.84 \pm 0.3$. However, KP03 still adopted $\alpha = 1$ when they used the EW R_{23} to estimate the oxygen abundances of galaxies.

4. Analysis of emission-line quantities

Several relations are analyzed in this section, including those of the emission-line quantities, e.g. $EW(H\beta)$, with the α parameter, with the discrepancies of EW R_{23} and flux R_{23} , and with the discrepancies of the $\log(O/H)$ abundances derived from these two R_{23} values.

4.1. Relations between the line strengths and α parameters

Figure 2a shows the relations between the emission-line strengths $EW(H\beta)$ and the line-ratio $\frac{EW_{[\text{O III}]} / I_{[\text{O III}]}}{EW_{H\beta} / I_{H\beta}}$ ($=1/\alpha$) of the sample galaxies. The solid line marks the one-to-one correspondence. It seems that there is some correlation between the α parameter and the emission-line strengths: from the galaxies with stronger emission lines, the ratios of $\log(\frac{EW_{[\text{O III}]} / I_{[\text{O III}]}}{EW_{H\beta} / I_{H\beta}})$ ($=\log(1/\alpha)$) change from -0.2 (mostly) to 0.5 monotonically, though the scatter is large and show some exceptional points with $\log(1/\alpha) < -0.2$. This range is similar to what KP03 found for their sample galaxies. The line strengths of [O II] and [O III], i.e., $EW_{[\text{O II}]}$ and $EW_{[\text{O III}]}$, also show similar trends to $EW(H\beta)$ in these kinds of relations, but with somewhat larger scatter. The ratio $\log(\frac{EW_{[\text{O II}]} / I_{[\text{O II}]}}{EW_{H\beta} / I_{H\beta}})$ ($=\log(1/\alpha)$) of all the sample galaxies show a median value of 0.069 dex (with a scatter of 0.060 dex) and a mean value of 0.077 dex (with a scatter of 0.104 dex).

4.2. Discrepancies between EW R_{23} and R_{23}

When directly using the EW R_{23} to replace the flux R_{23} , namely, $\alpha=1$ is adopted for EW R_{23} , the derived metallicities could have some discrepancies. Figure 2b shows the discrepancies between the EW R_{23} and the extinction-corrected flux R_{23} as a function of line strengths $EW(H\beta)$. The general trend is that, from galaxies with stronger line strengths, the differences between $\log(EW R_{23})$ and $\log(R_{23})$ increase from -0.15 (mostly) to 0.5 dex monotonically. KP03 also find a similar trend for their sample galaxies. Our much larger sample shows this systematic discrepancy more clearly. The median value of these discrepancies is about 0.061 dex (with a scatter of 0.050 dex), and the mean value of them is about 0.069 dex (with a scatter of 0.086 dex).

4.3. Discrepancies between $(O/H)_{EW R_{23}}$ and $(O/H)_{R_{23}}$

One of the most important results of this work is given in Fig. 2c, which shows the difference between $\log(O/H)_{EW R_{23}}$ and

$\log(O/H)_{R_{23}}$ as functions of the emission-line strengths $EW(H\beta)$. The general trend is that, from the galaxies with stronger line strengths, the differences in the two $\log(O/H)$ estimates change from -0.5 to 0.2 dex, with most of them ranging from -0.2 to 0.1 dex. KP03 do not present such a direct comparison for the O/H abundances.

The large sample of SDSS star-forming galaxies that we use generally show that the EW R_{23} will underestimate the oxygen abundances of the sample galaxies by a factor of 0.041 (the median offset, with a scatter of 0.036 dex) or 0.054 dex (the mean offset, with a scatter of 0.078 dex). Here the $\log(O/H)$ abundances were obtained from the R_{23} calibration of Tremonti et al. (2004). We also adopted some other R_{23} calibration formulas, i.e. Kobulnicky et al. (1999, the analysis formulas for the models of McGaugh 1991), Zaritsky et al. (1994), and Kobulnicky & Kewley (2004, the average of McGaugh 1991 and Kewley & Dopita 2002), to check these discrepancies, the results of which are quite similar. Moustakas & Kennicutt (2006) find similar discrepancies to ours by comparing the abundances derived from the extinction-corrected flux- and EW- R_{23} of 12 nearby spiral galaxies. They find that the integrated abundances determined from the emission-lines systematically underestimated the characteristic abundances. The mean offset is -0.06 ± 0.09 dex using the McGaugh (1991) calibration, or -0.11 ± 0.13 dex using the Pilyugin & Thurán (2005) calibration, and the corresponding median offsets are -0.04 and -0.09 dex, respectively.

These results show that the oxygen abundances derived from the EW R_{23} and the extinction-corrected flux- R_{23} are not seriously different for these star-forming galaxies, generally less than 0.1 dex. However, the global discrepancy of them does show a wide distribution, from -0.5 to 0.2 dex, which means that this replacement of EW R_{23} to flux R_{23} for metallicity estimates could cause different effects on the individual galaxies, and should be considered carefully.

5. Modifying the EW R_{23} -method

It is interesting to further check the main factors that affect the discrepancy between the $\log(O/H)$ abundances derived from EW R_{23} and flux R_{23} . We may then find some ways to modify the EW R_{23} method in order to obtain almost identical oxygen abundances to the flux R_{23} on the basis of this large set of SDSS galaxies.

5.1. Factors that affect the α parameter

In Sect.3, we point out that the α parameter is the ratio of the intrinsic continua underlying [O II] $\lambda 3727$ and $H\beta$ and that it is related to the observed continua and the line extinction c (see Eq. (5)). In this section, we discuss the dominant effect on the α parameter.

Equation (5) shows α is a function of the dust extinction and stellar populations of the galaxies, so then we have

$$\begin{aligned} \alpha &= \frac{F_{C, [\text{O II}]}}{F_{C, H\beta}} 10^{c(f([\text{O II}]) - f(H\beta))} \\ &= \frac{F_{C, [\text{O II}]}}{F_{C, H\beta}} 10^{(c-c^*)(f([\text{O II}]) - f(H\beta))}, \end{aligned} \quad (6)$$

where $F_{C, [\text{O II}]}$ and $F_{C, H\beta}$ are the dereddened continua underlying [O II] and $H\beta$, c the dust attenuation on emission-line, and c^* characterizes the dust attenuation on the continuum. Here we assume c^* and c follow the same reddening law. (Also see KP03)

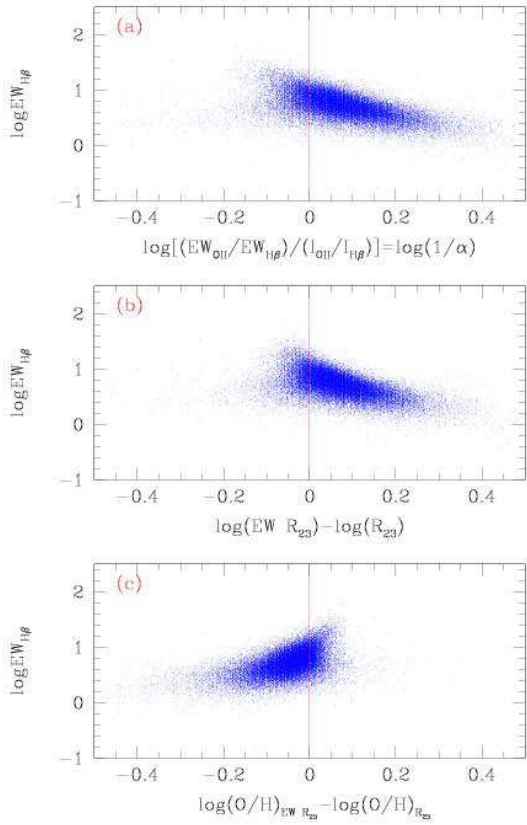


Fig. 2. (a). Emission-line strengths $EW(H\beta)$ of the sample galaxies as a function of the ratios of equivalent width ratios to dereddened emission-line fluxes ratios for $[O\ II]/H\beta$. (b). $EW(H\beta)$ as a function of the discrepancy between the quantity of $EW R_{23}$ and the flux R_{23} (extinction-corrected). (c). $EW(H\beta)$ as a function of the discrepancy between the two metallicity estimates from $EW R_{23}$ and flux R_{23} .

As a rough estimate, we assume that the sample galaxies follow the same extinction law as the starburst galaxies studied by Calzetti et al. (1994), who found that the difference between the optical depths of the continua underlying the Balmer lines is about one-half of the difference between the optical depths of the Balmer emission lines (their Eq.26). Thus, we assume $c^* \approx 0.5c$, and then obtain the following equation:

$$\alpha = \frac{F_{C,[OII]}^0}{F_{C,H\beta}^0} 10^{0.5c(f([OII]) - f(H\beta))}, \quad (7)$$

where $F_{C,[OII]}^0/F_{C,H\beta}^0$ characterizes the stellar populations of the galaxies, and c -term characterizes the dust extinction.

It is easy to check the relation between α and the dust extinction c since we have obtained both of them for the individual galaxies. However, we cannot obtain the intrinsic values of $F_{C,[OII]}^0/F_{C,H\beta}^0$ directly. Fortunately, the MPA/JHU group and the SDSS provide $D_n(4000)$ parameters and several photometric magnitudes for this large sample of galaxies, which can characterize the stellar populations of the galaxies. We check the relations between α and dust extinction c , $D_n(4000)$, $g-r$ colors for the sample galaxies in the next three sections.

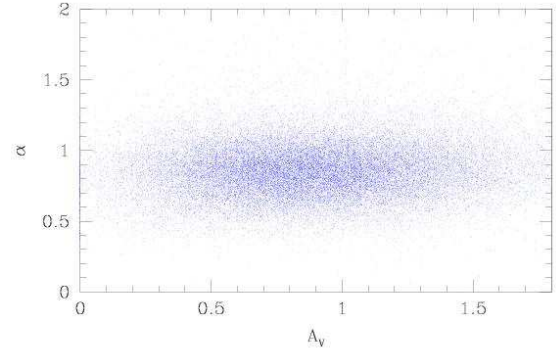


Fig. 3. Relation of α parameter and dust extinction A_V for the sample galaxies.

5.2. The relation between α and dust extinction

The $[O\ II]\lambda 3727$ is bluer in wavelength and is affected more strongly by dust extinction than $H\beta$, thus the α parameter may be correlated with dust extinction A_V . Figure 3 shows the α parameter as a function of dust extinction $A_V (=cR_V/1.47, \text{Seaton (1979), } R_V=3.1)$. The derived A_V is from 0 to 2.7, with the median and average values of 0.87 and 0.89, respectively. It shows that there is no clear correlation between α and A_V for these SDSS sample galaxies, and the linear least-square fit is $\alpha = 0.056A_V + 0.821$ with a very slight slope. This means that the differences in the continua underlying $[O\ II]\lambda 3727$ and $H\beta$ are not affected much by dust extinction. The reasons may be that the related two lines are not very far away at wavelength and that the dust extinction coefficients of these SDSS star-forming galaxies are not so large.

5.3. The corrected $EW R_{23}$ method using $D_n(4000)$ index

The break occurring at 4000\AA is the strongest discontinuity in the optical spectrum of a galaxy, and it arises because of the accumulation of a large number of spectral lines in a narrow wavelength region. The main contribution to the opacity comes from ionized metals. In hot stars, the elements are multiply ionized and the opacity decreases, so the 4000-\AA break will be small for young stellar populations and large for old, metal-rich galaxies (Kauffmann et al. 2003). Kauffmann et al. (2003) adopt the narrow definition from Balogh et al. (1999) and denote this index as $D_n(4000)$ for the SDSS galaxies. It is the ratio of the average flux density F_ν in the bands $3850\text{-}3950$ and $4000\text{-}4100\text{\AA}$, 100\AA narrower than the definition by Bruzual (1983). The parameter $D_n(4000)$ is one of the main ones used by Kauffmann et al. (2003) to trace the stellar formation history of the SDSS galaxies, which shows a monotonic increase after the instantaneous burst of star formation.

We plot the relations of α against $D_n(4000)$ for the sample galaxies in Fig. 4a, which clearly shows a correlation. A third-order polynomial fit for this relation is obtained by fitting the 16 median-value points in bins of 0.05 in $D_n(4000)$ from 1 to 1.8, and given as:

$$\alpha = 10.88 - 18.31x + 11.18x^2 - 2.34x^3, \quad (8)$$

with a standard error of 0.164, where $x = D_n(4000)$. This relation of α vs. $D_n(4000)$ could be used to correct the $EW R_{23}$ and then to obtain the consistent metallicities of galaxies with the flux R_{23} . We propose using $R_{23}(EW)_{\text{corrected}} =$

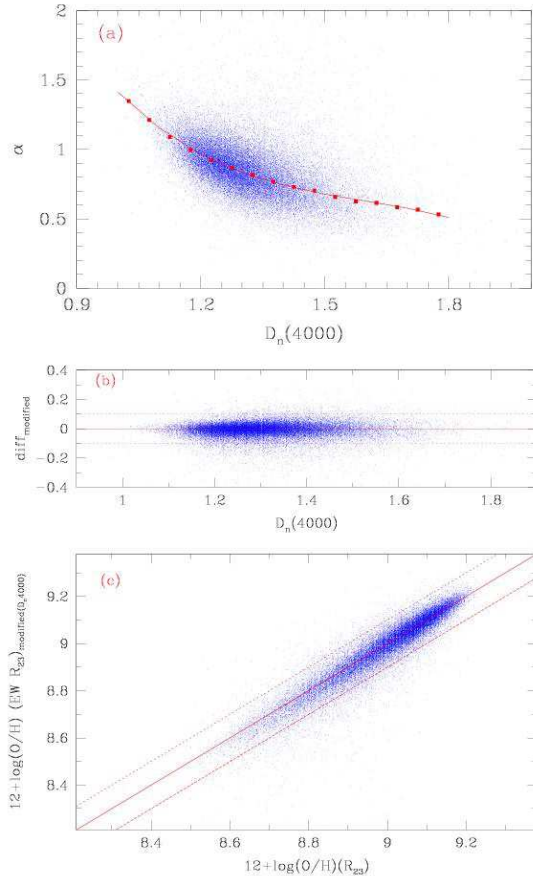


Fig. 4. (a). Relation of the α and $D_n(4000)$ parameters for the sample galaxies. The big squares are the 16 median-value points in the bins of 0.05 in $D_n(4000)$ from 1.0 to 1.8. The solid line represents the third-order polynomial fit for these median-value points, and it is given as Eq. (8). (b). Comparison between the metallicities derived from the α -modified EW R_{23} by using $D_n(4000)$ following Eq. (8) (marked as the subscript “modified”). The *diff* refers to the difference between the oxygen abundances from the modified EW R_{23} and flux R_{23} . (c). The direct comparison between the two oxygen abundances derived from the modified EW R_{23} and flux R_{23} (extinction-corrected). In (b) and (c), the solid lines are the equal-value lines, and the dashed lines show the 0.1 dex discrepancy.

$\alpha \times EW([\text{O II}])/EW(\text{H}\beta) + EW([\text{O III}])/EW(\text{H}\beta)$ to then estimate the metallicities of galaxies.

Figure 4b shows the consistency of the metallicity estimates from the corrected EW R_{23} and flux R_{23} after we apply the correction of $D_n(4000)$ for α . Figure 4c shows more direct comparisons for the two O/H estimates with such a correction. Both of them show that the two derived abundances are very consistent. The median and mean discrepancies between $\log(\text{O}/\text{H})_{EW R_{23}}$ and $\log(\text{O}/\text{H})_{R_{23}}$ now decrease to about -0.005 dex (with a scatter of 0.024 dex), and -0.010 dex (with a scatter of 0.054 dex), respectively. Then the corrected EW R_{23} method provides $\log(\text{O}/\text{H})$ abundances similar to those of the extinction-corrected flux R_{23} method within an accuracy of ± 0.1 dex for $>94\%$ of the galaxies.

Unfortunately this correction is difficult to handle with non-calibrated spectra, simply because reliable measurements for $D_n(4000)$ require flux-calibrated spectroscopy. Since $D_n(4000)$ amplitude depends on the stellar population, age, and metallic-

ity, it also correlates with colors. In the following we aim at generating a correction usable by a large community, using a non-calibrated spectrum and one color as input (e.g. $g - r$ for the SDSS data).

5.4. The corrected EW R_{23} method using $g - r$ color

Colors can provide important information for the stellar populations of the galaxies and can be obtained directly from the photometric observations. SDSS has made the u, g, r, i, z band magnitudes of the galaxies available publicly. Since the u magnitude has large uncertainty (20 per cent; Kauffmann et al. 2003) and the images in u - and z -band are relatively shallow, whereas i -band image may suffer from the ‘red halo’ effect (Michard 2002; Wu et al. 2005), we use $g - r$ color here to study such corrections for α . The g and r magnitudes can be converted to other band magnitudes, e.g. B, V , following some conversions, for example, Smith et al. (2002) and Jordi et al. (2006).

Figure 5a shows the correlation between the $g - r$ colors (in Petrosian magnitudes) and α for the sample galaxies. The basic trend shows that the redder galaxies have relatively lower α values, corresponding to the larger differences between the underlying continua of $[\text{O II}]$ and $\text{H}\beta$. The third-order polynomial fits for these correlations were obtained and given as

$$\alpha = 1.20 - 1.11 x + 1.15 x^2 - 0.53 x^3, \quad (9)$$

with a standard error of 0.186, where x refers to $g - r$ color. Then we propose using $R_{23}(EW)_{corrected} = \alpha \times EW([\text{O II}])/EW(\text{H}\beta) + EW([\text{O III}])/EW(\text{H}\beta)$ to estimate the metallicities of galaxies.

Figure 5b shows the consistency of the metallicity estimates from the corrected EW R_{23} and flux R_{23} after we apply the correction from $g - r$ color for α . Figure 5c shows the comparison between the two O/H estimates with this correction more directly. They show that the median and mean discrepancies between $\log(\text{O}/\text{H})_{EW R_{23}}$ and $\log(\text{O}/\text{H})_{R_{23}}$ now decrease to about -0.004 dex (a scatter of 0.030 dex) and -0.012 dex (a scatter of 0.062 dex), respectively. Then the two oxygen abundance estimates are almost identical to each other. Namely, the corrected EW R_{23} method provides $\log(\text{O}/\text{H})$ abundances similar to those of the extinction-corrected flux R_{23} method within an accuracy of ± 0.1 dex for $>92\%$ of the galaxies.

5.5. Correction for the EW R_{23} method by a constant $\alpha=0.85$

The calculated median α value of this large sample of SDSS local star-forming galaxies is about 0.85 (the average value is ~ 0.86). We may also use this constant α -factor to modify the EW R_{23} . However, this constant correction is only useful for estimating the global metallicity distribution of a large dataset, for example, from the database of a survey. As for the individual galaxy, this may reversely enlarge the uncertainty for some of them, for example, the object with about $EW(\text{H}\beta) \sim 10\text{\AA}$ (see Fig. 2a). Indeed, the correction on EW R_{23} for the individual galaxies correlates tightly with their stellar populations and star formation histories.

6. Discussions about the boundary of the upper branch of $12 + \log(\text{O}/\text{H})$

In this work, we adopt $12 + \log(\text{O}/\text{H}) \sim 8.5$ as the low boundary of the upper branch of oxygen abundances from the $\log R_{23}$ calibration. The main reason is that the R_{23} calibration used (taken from Tremonti et al. 2004) is valid above this metallicity. In Sect. 6.1,

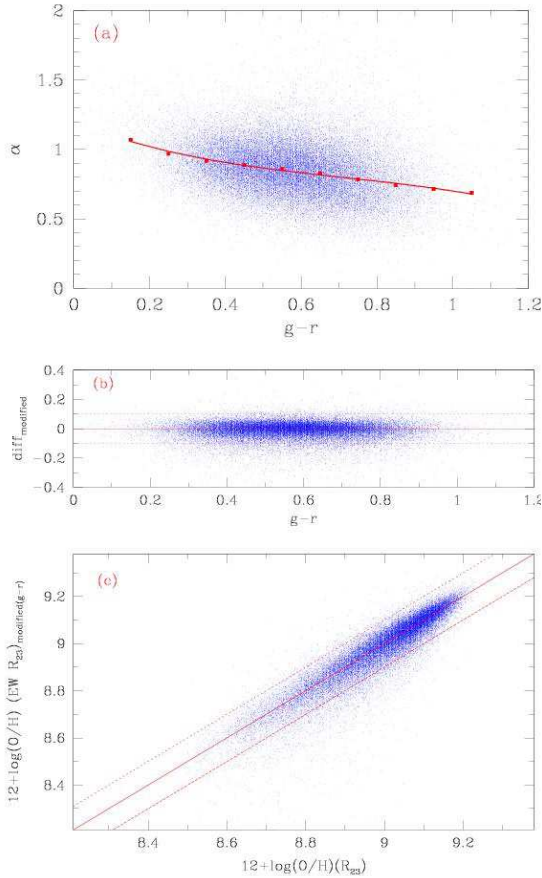


Fig. 5. (a). Relation of the α and $g-r$ colors for the sample galaxies. The big squares refer to the 10 median-value points in the bins of 0.1 in $g-r$ from 0.1 to 1.1. The solid line represents the third-order polynomial fit for these median-value points, and it is given by Eq. (9). (b). Comparison between the metallicities derived from the α -modified EW R_{23} by using $g-r$ colors following Eq. (9) (marked as the subscript “modified”). The “*diff*” is as a function of $g-r$ colors. (c). The direct comparison between the two oxygen abundances from the α -modified EW R_{23} and the flux R_{23} (extinction-corrected). The solid lines are the equal-value lines, and the dashed lines show the 0.1 dex discrepancy from the equal-value lines in (b) and (c).

we present more observational data with O/H abundances derived from electron temperature T_e , especially from the recent SDSS, and some photoionization models to further identify the reason we adopt $12+\log(\text{O}/\text{H})\sim 8.5$ as the boundary of the upper branch of oxygen abundances to compare the EW R_{23} and flux R_{23} methods. However, this boundary value is a bit higher than used by some other researchers, e.g., Pilyugin (2000, 2001a,b) and Pilyugin & Thuan (2005), who use $12+\log(\text{O}/\text{H})\sim 8.2$ on the basis of a sample of H II regions having their $\log(\text{O}/\text{H})$ abundances estimated from T_e . Therefore, we extend the boundary to compare the EW R_{23} and flux R_{23} methods and check whether our relations are valid or not in the region of $12+\log(\text{O}/\text{H})_{T_e}\sim 8.2-8.5$, which will be presented in Sect. 6.2.

6.1. The observational data with $(\text{O}/\text{H})_{T_e}$ and the photoionization models

In Fig. 6a we plot the $(\text{O}/\text{H})_{T_e}$ - R_{23} relations for the sample galaxies having T_e -based O/H abundances, which are taken from

Kniazev et al. (2004, 624 samples), Izotov et al. (2006, 409 samples), and Yin et al. (2007, 695 samples). Figure 6b presents the predictions of photoionization models for the relations of $12+\log(\text{O}/\text{H})$ vs. $\log R_{23}$ taken from Kewley & Dopita (2002) and Kobulnicky et al. (1999, K99), which was obtained by analyzing those of McGaugh (1991).

Figure 6a and Fig. 6b show that both the large sample of observational data and photoionization models confirm that it is very difficult to derive a reliable O/H abundance from the R_{23} parameter for the region of $12+\log(\text{O}/\text{H})<8.5$ because of the large scatter of the data points there, the weak dependence of O/H on R_{23} (down to $12+\log(\text{O}/\text{H})<7.9$), and the strong effects of ionization parameters. Yin et al. (2007) has used their Fig.3b to show the large discrepancy, up to 0.4 dex, of the two sets of $\log(\text{O}/\text{H})$ estimates derived from the upper branch and lower branch of R_{23} calibrations for the samples within $7.9<12+\log(\text{O}/\text{H})<8.4$. Stasinska (2002) discusses the weak dependence of (O/H) on R_{23} in the transition region from nebular physics.

Considering the discussions above, and also to avoid that some galaxies included may lie in the lower branch of the R_{23} -(O/H) relation, we select the galaxies having $12+\log(\text{O}/\text{H})>8.5$ to check the EW R_{23} method in this study. However, it could be useful to check this and the validity of our relations in an extended upper branch range, $12+\log(\text{O}/\text{H})\sim 8.2-8.5$, as used in some studies.

6.2. Checking the extended upper-branch range of $12+\log(\text{O}/\text{H})\sim 8.2-8.5$

We select a subsample from Fig. 6a to check the situation in the extended range of upper branch, $12+\log(\text{O}/\text{H})\sim 8.2-8.5$. To be consistent with other parts of this work, we select this subsample based on the SDSS-DR2 catalog. Finally, 37 independent objects with metallicities of $8.2<12+\log(\text{O}/\text{H})_{T_e}<8.5$ are selected by cross-correlating the DR2 catalog with the lists of Kniazev et al. (2004, from DR1), Izotov et al. (2006, from DR3), and Yin et al. (2007, from DR4). Then we use the EW and flux measurements of the related emission lines provided by the MPA/JHU group to estimate their EW R_{23} and flux R_{23} , hence, the resulted abundances.

These 37 galaxies show a discrepancy between $\log(\text{EW}R_{23})$ and $\log(R_{23})$ (as Fig. 2b) within a range of -0.2 to 0, which may result in overestimated $\log(\text{O}/\text{H})$ abundances of about 0-0.2 dex by the $\text{EW}R_{23}$ as shown in Fig. 2c. Their $D_n(4000)$ values are around 1.0, with $g-r$ colors around 0.0 (ranging from -0.2 to 0.3), which confirms that they are low-metallicity objects that will distribute in the left hand parts in Figs. 4a and 5a. Their α values are within 1-2, with the average value about 1.5. If we apply the α corrections for their EW R_{23} , the correction factors will be about $\alpha\sim 1.4$ and 1.2 by extrapolating Eqs. (8) and (9), respectively.

If we do not consider the discrepancy among the different photoionization parameters and the weak dependence of O/H on R_{23} in this metallicity region (shown as Fig.6b) and try to extrapolate the R_{23} calibration of Tremonti et al. (2004) down to these objects with $8.2<12+\log(\text{O}/\text{H})_{T_e}<8.5$, then the open squares in Fig. 7a show that the R_{23} method will often overestimate the abundances of the galaxies and even underestimate the abundances of some galaxies. The stars in Fig.7a show that the EW R_{23} method provides a higher $\log(\text{O}/\text{H})$ abundance than the flux R_{23} , generally about 0.2 dex, which is consistent with the discussions above and with Fig.2c. Figure 7a also shows that the correction by $\alpha(g-r)$ will not improve the consistency for these objects much, and the correction by

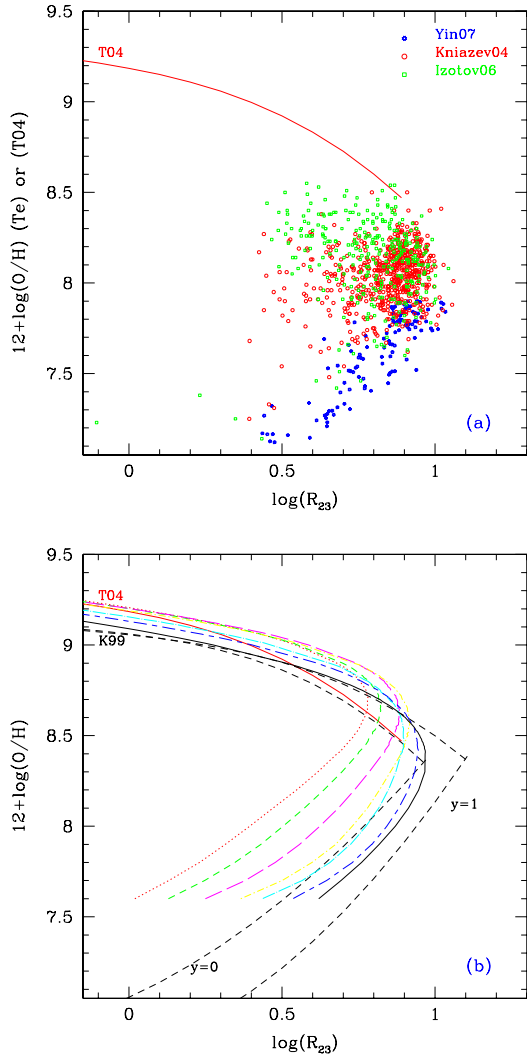


Fig. 6. (a). The T_e -based abundances and $\log R_{23}$ of the galaxies and H II regions taken from Yin et al. (2007, Yin07), Kniazev et al. (2004, Kniazev04), and Izotov et al. (2006, Izotov06). Associated with the calibration from SDSS-DR2 observations given by Tremonti et al. (2004; the thick solid line, marked by 'T04'). (b). The predictions of photoionization models for the relations of $12+\log(\text{O}/\text{H})$ vs. $\log(R_{23})$: the two dashed lines marked with y values are taken from Koblunicky et al. (1999, K99), which are the analytical formulas for McGaugh (1991); the seven thin lines down to $12+\log(\text{O}/\text{H})\sim 7.6$ are taken from Kewley & Dopita (2002) with different ionization parameter q values. The thick solid line is the same as (a). Both (a) and (b) show that it is very difficult to derive the reliable O/H abundance from the R_{23} parameter for the cases of $12+\log(\text{O}/\text{H})<8.5$. (See the online color versions of the plots for the discrepancies of the data and models.)

$\alpha(D_n(4000))$ gives more consistent O/H abundances for the objects with $12+\log(\text{O}/\text{H})_{R_{23}}>8.2$. We changed to the R_{23} calibration of Zaritsky et al. (1994) (which is an average of three previous calibrations) to obtain these comparisons again, and find the results are very similar to Fig. 7a.

We also used the R_{23} calibration of Pilyugin (2000) (their Eq.5) to do these comparisons, and present the results in Fig. 7b. It shows that mostly the flux R_{23} method provides consistent $\log(\text{O}/\text{H})$ abundances with the T_e method, except for some data

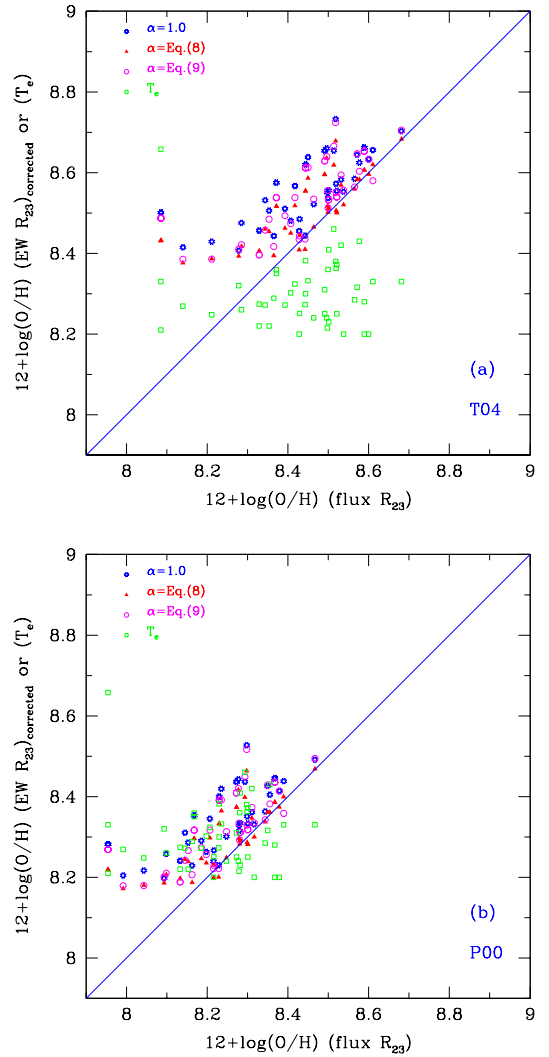


Fig. 7. Comparisons between the $\log(\text{O}/\text{H})$ abundances obtained from flux R_{23} and those from T_e or from the corrected or uncorrected EW R_{23} method: (a) using the R_{23} calibration of Tremonti et al. (2004, T04); (b) using the R_{23} calibration of Pilyugin (2000, P00). The different symbols represent those what obtained from the different methods marked by the labels in the top left corner.

points in the left hand part of the data with underestimated $\log(\text{O}/\text{H})_{R_{23}}$ and some reversed ones in the right hand section. It also shows that the corrected EW R_{23} method by $\alpha(D_n(4000))$ provides more consistent abundances with the flux R_{23} for the objects with $12+\log(\text{O}/\text{H})_{R_{23}}>8.1$ than the uncorrected EW R_{23} or corrected by $\alpha(g-r)$, which are similar to Fig. 7a. These differences among the EW R_{23} abundances presented in Fig. 7 are not difficult to understand since the average α value of these low-metallicity objects is about 1.5, which is higher than the correction relations provided, ~ 1.4 or 1.2 .

In short, in the lower metallicity range of $8.2 < 12+\log(\text{O}/\text{H})_{T_e} < 8.5$, we would not recommend using our relations to correct the EW R_{23} method for the oxygen abundance calibrations, since there are several situations affecting the results, such as the big scatter of the data, the strong effects of ionization parameters, and the weak dependence of O/H on R_{23} in the range.

7. Summary and conclusion

The goal of this paper is to check the reliability of using EW R_{23} ($=\frac{EW([OII])+EW([OIII])}{EW(H\beta)}$) to replace the extinction-corrected flux R_{23} ($=\frac{I([OII])+I([OIII])}{I(H\beta)}$) to estimate the metallicities of star-forming galaxies on the basis of a large sample (37,173) of galaxies with $12+\log(O/H)_{R_{23}}>8.5$, selected from the SDSS-DR2. This replacement is often adopted when there are some problems dealing with proper flux calibrations for the spectral observations. This large sample can provide some obvious statistical trends.

The results show that the logarithm values of EW R_{23} and extinction-corrected flux- R_{23} have a discrepancy from -0.4 to 0.5 dex, with a median value of about $+0.061$ dex and a mean value about $+0.069$ dex. Thus, the discrepancies between the $\log(O/H)$ abundances obtained from EW R_{23} and those from the flux- R_{23} range from -0.5 to 0.2 dex and have a median value of about -0.041 dex, a mean value of about -0.054 dex. These discrepancies are caused by the different continua ($F_{C\lambda}$) underlying the emission lines [O II] and H β ([O III], as well). These differences are characterized by the α parameter as $(F_{C,H\beta})/(F_{C,[OII]})$, which changes from 0.1 to 2.6, and by a median value of 0.85 and a mean value of 0.86.

Then we discuss the factor that affects this discrepancy mostly. Our large sample of data shows that the α parameter is almost independent of the dust extinction inside the galaxies and depends closely on stellar populations of the galaxies, which can be quantified by the $D_n(4000)$ parameters and colors of the galaxies. Third-order polynomial fits have been obtained for the observed relations of α versus $D_n(4000)$ and α versus $g-r$ colors for the sample galaxies, which can be used to modify the EW R_{23} method. After applying this correction by $D_n(4000)$, the median and mean discrepancies between $\log(O/H)_{EW R_{23}}$ and $\log(O/H)_{R_{23}}$ decrease to about -0.005 dex and -0.010 dex, respectively. After applying this correction by $g-r$ colors, the median and mean discrepancies between $\log(O/H)_{EW R_{23}}$ and $\log(O/H)_{R_{23}}$ decrease to about -0.004 dex and -0.012 dex, respectively. The two derived sets of $\log(O/H)$ abundances are almost identical now.

In summary, when there are problems with flux calibrations of the spectra, the EW R_{23} could be used roughly to replace the extinction-corrected flux R_{23} to estimate the metallicities of star-forming galaxies. The discrepancy caused by this replacement can be from -0.2 to 0.1 dex generally. This factor is consistent with those found by KP03 and Moustakas & Kennicutt (2006). However, this discrepancy could be large for the different individual galaxies, from -0.5 to 0.2 , if the underlying continua of [O II] and H β ([O III]) are quite different. The $D_n(4000)$ parameters and colors of the galaxies are very useful for correcting the EW R_{23} method, which will then greatly decrease the discrepancies and result in an almost identical oxygen abundance to the flux- R_{23} .

Nevertheless, the modified EW R_{23} still suffers from the drawback of the “double-value” of R_{23} for the O/H estimates, and some other strong-line ratios are also useful for estimating the metallicities of galaxies then, such as [N II]/H α , ([O III]/H β)/([N II]/H α), [N II]/[S II] and [O III]/H β , etc. (Kewley & Dopita 2002; Pettini & Pagel 2004; Liang et al. 2006; Yin et al. 2007).

Acknowledgments

We thank our referee for the valuable comments and suggestions, which helped to improve this work. We thank Rob

Kennicutt, Lisa Kewley, Hong Wu, Licai Deng, Bo Zhang, and Hector Flores for valuable discussions related to this study, and thank Ruixiang Chang, Shiyang Shen, Caina Hao, Jing Wang, and Chen Cao for helpful discussions about the SDSS database. We thank James Wicker for his help in improving the English expression in the text. This work was supported by the Natural Science Foundation of China (NSFC) Foundation under No.10403006, 10433010, 10673002, 10573022, 10333060, and 10521001; and the National Basic Research Program of China (973 Program) No.2007CB815404.

References

- Abazajian, K., Adelman-McCarthy, J.K., Agueros, M.A. et al. 2004, AJ, 128, 502
- Balogh, M. L., Morris, S.L., Yee, H.K.C., Carlberg, R.G., Ellingson, E., 1999, ApJ, 527, 54
- Brinchmann, J., Charlot, S., White, S. D. M., Tremonti, C., Kauffmann, G., Heckman, T., Brinkmann, J., 2004, MNRAS, 351, 1151
- Bruzual, A. G., 1983, ApJ, 273, 105
- Calzetti, D., Kinney, A. L., Storchi-Bergmann, T., 1994, ApJ, 429, 582
- Izotov, Y. I., Stasinska, G., Meynet, G. et al. 2006, A&A, 448, 955
- Jordi, K., Grebel, E. K., Ammon, K., 2006, A&A, 460, 339
- Kauffmann, G., Heckman, T.M., White, S.D.M. et al. 2003, MNRAS, 341, 33
- Kobulnicky, H. A., Kennicutt, R.C.Jr., & Pizagno, J.L., 1999, ApJ, 514, 544
- Kobulnicky, H. A., Kewley, L.J., 2004, ApJ, 617, 240
- Kobulnicky, H. A., Willmer, C.N.A., Phillips, A. C. et al. 2003, ApJ, 599, 1006
- Kobulnicky, H. A., Phillips, A.C., 2003, ApJ, 599, 1031 (KP03)
- Kewley, L. J. & Dopita, M. A. 2002, ApJS 142, 35
- Kniazev, A. Y., Pustilnik, S. A., Grebel, E. K. et al. 2004, ApJS, 153, 429
- Lamareille, F., Contini, T., Le Borgne, J.-F. et al. 2005a, A&A, 448, 893
- Lamareille, F., Contini, T., Brinchmann, J. et al. 2005b, A&A, 448, 907
- Liang, Y. C., Yin, S. Y., Hammer, F. et al. 2006, ApJ, 652, 257
- McGaugh, S. S. 1991, ApJ, 380, 140
- Michard, R. 2002, A&A, 384, 763
- Mouchine, M., Bamford, S. P., Aragon-Salamanca, A. et al. 2006a, MNRAS, 368, 1871
- Mouchine, M., Bamford, S. P., Aragon-Salamanca, A. et al. 2006b, MNRAS, 369, 891
- Moustakas, J. & Kennicutt, R. C. Jr., 2006, ApJ, 651, 155
- Osterbrock, D. E., 1989, Astrophysics of Gaseous Nebulae and Active Galactic Nuclei. Mill Valley, California University Science BookS
- Pagel, B. E. J., Edmunds, M. G., Blackwell, D. E. et al. 1979, MNRAS, 189, 95
- Pagel, B. E. J., Simonson, E.A., Terlevich, R.J., Edmunds, M.G., 1992, MNRAS, 255, 325
- Pettini, M. & Pagel, B. E. J., 2004, MNRAS, 348, L59
- Pilyugin, L. S., 2000, A&A, 362, 325
- Pilyugin, L.S., 2001a, A&A, 369, 594
- Pilyugin, L.S., 2001b, A&A, 373, 56
- Pilyugin, L. S. Thuan, T. X., 2005, ApJ, 631, 231
- Seaton, M. J., 1979, MNRAS, 187, 73
- Skillman, E. D., & Kennicutt, R.C.Jr., 1993, ApJ, 411, 655
- Smith, J. A., Tucker, D. L., Kent, S. et al., 2002, AJ, 123, 2121
- Stasinska, G. 2002, astro-ph/0207500
- Strauss, M. A., Weinberg, D.H., Lupton, R.H., 2002, AJ, 124, 1810
- Tremonti, C. A. et al. 2004, ApJ, 613, 898
- Wu, H., Shao, Z. Y., Mo, H. J., Xia, X. Y., & Deng, Z. G. 2005, ApJ, 622, 244
- Yin, S.Y., Liang, Y.C., Hammer, F. et al. 2007, A&A, 462, 535
- Zaritsky, D., Kennicutt, R. C., Huchra, J. P., 1994, ApJ, 420, 87